

## Article

# Photovoltaic/Thermal Module Integrated with Nano-Enhanced Phase Change Material: A Numerical Analysis

Yuanlong Cui <sup>1,\*</sup>, Jie Zhu <sup>2</sup> , Stamatis Zoras <sup>3</sup>, Khalid Hassan <sup>2</sup> and Hui Tong <sup>1,\*</sup>

<sup>1</sup> School of Architecture and Urban Planning, Shandong Jianzhu University, 1000 Fengming Road, Jinan 250101, China

<sup>2</sup> Department of Architecture and Built Environment, University of Nottingham, Nottingham NG7 2RD, UK; jie.zhu@nottingham.ac.uk (J.Z.); alykh5@nottingham.ac.uk (K.H.)

<sup>3</sup> Department of Built Environment, College of Engineering and Technology, University of Derby, Derby DE22 3AW, UK; s.zoras@derby.ac.uk

\* Correspondence: cuiyuanlong22@sdjzu.edu.cn (Y.C.); rover@sdjzu.edu.cn (H.T.)

**Abstract:** Solar photovoltaic-thermal (PV/T) technology is the main strategy for harvesting solar energy due to its non-polluting, stability, good visibility and security features. The aim of the project is to develop a mathematical model of a PV/T module integrated with optical filtration and MXene-enhanced PCM. In this system, a single MXene-enhanced PCM layer is attached between the PV panel and absorber pipe with solid MXene-PCM for storage and cooling purposes. Additionally, the thermal fluid is utilized in the copper absorber pipe and connected to the heat pump system for enhancing system thermal and electrical efficiency. Furthermore, the influences of the optical filtration channel height, concentration of the nanoparticles on PV surface temperature and overall system efficiency are also discussed. This study demonstrates that the annual thermal and electrical energy output can reach 5370 kWh per annum with 74.92% of thermal efficiency and 5620 kWh with 14.65% of electrical efficiency, respectively, compared to the traditional PV/T module. Meanwhile, when the optical filtration channel height and volume concentration are enhanced, they exert a negative influence on the PV surface temperature, but the overall thermal efficiency is enhanced due to low thermal resistance to heat losses and low radiation-shielding layers.

**Keywords:** PV/T module; optical filtration; nano-enhanced PCM; thermal and electrical output; thermal and electrical efficiency



**Citation:** Cui, Y.; Zhu, J.; Zoras, S.; Hassan, K.; Tong, H. Photovoltaic/Thermal Module Integrated with Nano-Enhanced Phase Change Material: A Numerical Analysis. *Energies* **2022**, *15*, 4988. <https://doi.org/10.3390/en15144988>

Academic Editor: Sheikh Khaleduzzaman Shah

Received: 30 April 2022

Accepted: 2 July 2022

Published: 7 July 2022

**Publisher's Note:** MDPI stays neutral with regard to jurisdictional claims in published maps and institutional affiliations.



**Copyright:** © 2022 by the authors. Licensee MDPI, Basel, Switzerland. This article is an open access article distributed under the terms and conditions of the Creative Commons Attribution (CC BY) license (<https://creativecommons.org/licenses/by/4.0/>).

## 1. Introduction

Recently, the world energy requirement has enhanced excessively owing to the development of the global economy. It is anticipated that there is an approximately 60% need for improvement in energy needs by 2030. The major contribution of environmental issues, such as climate change, air pollution and acid rain because of the consumption of fossil-based fuels, proves the dominance of renewable energy production sources in this regard. Currently, solar energy is thought of as the most promising and significant renewable energy source because it is clean, free and safe [1,2]. The efficiency of the PV panel is about 7–20% of solar energy conversion, nevertheless, the remaining 80% of solar radiation is waste heat and not electricity production [3,4] which results in an increase in the PV surface temperature and lifetime degradation of the PV cells. Hence, a combination of the photovoltaic panel and thermal collector as a unit to provide electricity and heat simultaneously is very popular in the field of solar energy. The operating temperature of the solar PV/T system could sustain a balance between the heat losses and heat obtained by the PV/T module. There are three key heat loss mechanisms including conduction, convection and radiation. To be more specific, heat conductive loss is attributed to the thermal gradients on the surface of the PV module and the absorber pipe arrangement. The

heat transfer ability of the PV/T module to the ambient environment depends on the thermal resistance, pipe configuration and PV cell materials. Heat convective transfer to solar PV/T modules is because of wind blowing across the PV surface and thermal fluid flow within the absorber pipe. Additionally, the heat conductive flow is analogous to the current conductive flow during the electrical power production period. The temperature difference is the driving force of heat conductive flow when the thermal resistance is constant, whereas when the PV module produces an electric circuit, it results in a voltage difference as the driving force of electrical power generation with a specific electrical resistance.

As for the solar PV/T module, one part is reflected into the ambient environment, another part is absorbed via the PV module itself as heat. The heating generated through the PV/T module is restricted which is attributed to the Shockley–Queisser limit. This will cause a high surface temperature in the PV array and a low energy conversion efficiency. Herein, a number of studies on the performance assessment of the PV/T unit have been explored. Specifically, Herrando et al. [5] set up a numerical model of PV/T unit to determine thermal and electricity production for a family building in the UK and obtained 36% space heating and 51% power. Huang et al. [6] performed a test on a PV/T unit and revealed that the system energy efficiencies can reach 35.33% for heat and 12.77% for power, respectively. Bianchini et al. [7] explored a commercial PV/T unit for providing thermal and electrical energy demands for a family building in Italy. It is found that the system can output 443 kWh/year of heat and 1362 kWh/year of electricity. Tang and Zhao [8] discovered a PV/T module with a micro channel system to investigate the entire performance and concluded that the pipe arrangement contributes to improving approximately 3% of electrical efficiency, resulting in an 8% decrease in PV surface temperature.

In order to increase the overall system efficiency, the optical filtration (OF) concept is introduced, for its unique characteristic to treat solar radiation before arriving at the PV modules. The PV module could convert a specific spectrum of solar radiation whereas the surplus part can be absorbed in the cells, resulting in overheating issues, which decreases the electrical energy output. Placing an OF in front of the PV module contributes to transmitting only the necessary portion for power generation; however, the remaining section is obtained by using the filtration fluid. Generally, liquid OF is able to transmit the wavelengths when the PV module is operated at high efficiency [9,10], which could help to obtain better electrical efficiency, reduce PV surface temperature, collect more thermal energy and extend the PV module lifetime for various types of applications. DeJarnette et al. [11] carried out an experimental investigation of a concentrating PV/T collector with a nanoparticle OF system and revealed that the solar transmission and absorbing rate are more than 75% and 80%, respectively. Han et al. [12] proposed a merit function to study the optical transmittance influence of PV/T with an OF system and obtained that valvoline oil and aqueous copper sulfate have lower optical transmittance than a normal system. Abdelrazik et al. [13] investigated experimentally the performance of solar PV/T with an OF system and analyzed the influence of silver nanoparticle concentrations and OF channel length on the optical properties of nanoparticle OF. It is found that the system could exhibit a better system conversion efficiency compared with the standalone PV system. Meanwhile, the optical transmittance is highly dependent on the volume concentration of the nanoparticles and OF channel length.

Additionally, nanofluids have exhibited outstanding enhancements in light of thermal and optical properties over conventional heat transfer fluids (HTFs) [14,15]. The utilization of nanofluids in PV/T is a recently innovated method to increase heat transfer properties. Adding nanomaterial to normal HTFs contributes to enhancing their optical and thermal properties [16–20]. Furthermore, the thermal and electrical output can be regulated by using the PV/T with a nanofluid system for meeting various demands [21–23]. In the meantime, the necessity of operational conditions based on the nanofluid spectral splitting technique is not very rigid because a conventional cleaning process has little influence on the performance of the OF [24,25]. For example, Yuan et al. [26] established mathematical equations of a PV/T with a PCM unit to study the energy conversion efficiency and

found that the system's electrical efficiency could be improved from 11.9% to 12.1%, by comparison, the thermal efficiency is reduced from 44.5% to 42.3%. Al-Waeli et al. [27,28] proposed a PV/T unit with a nano-enhanced PCM module and found that the electrical efficiency can be improved from 7.1% to 13.7% with an electrical output of 120.7 W, whereas the thermal energy output is 13.8 kW with an efficiency of 72%.

Lately, a novel family of two-dimensional (2D) graphene analogs consisting of transition metal carbides, carbonitrides and nitrides so-called "MXene",  $Ti_3C_2Tx$ , as the most typical representative, was explored, and great promise appears in the solar energy system owing to its high electrical and thermal conductivities, extraordinary optical absorption ability, unique 2D properties, such as graphene, non-toxicity, less corrosion and erosion, high surface area and rich surface hydrophilic heteroatoms [29,30]. Specifically, Fan et al. [31] explored the photo-to-thermal conversion and storage efficiency based on the composite MXene@ PEG nanomaterials and found that the maximum storage efficiency could reach 94.5% at the 20 wt% of MXene. To boost the photo-to-thermal conversion efficiency, Mo et al. [32] constructed the MXene@ PVA/PEG nanomaterials and revealed that the conversion efficiency could be 96.5% for 50 TPP and 87% for 70 TPP, respectively, indicating that the photo-to-thermal conversion efficiency is improved with the enhancement of MXene content. Samylingam et al. [33] simulated the thermal energy performance of a solar PV/T system integrated with the MXene@ olein palm oil (OPO) by using COMSOL software. The thermal efficiency of PV/T with MXene@ OPO could be enhanced by 11.2% in comparison to  $Al_2O_3$ -water nanofluid, in the meantime, the MXene@ OPO nanomaterial could supply an 8.5% improvement in heat removal from the PV/T thermal system, resulting in approximately 40% of the surface temperature reduction of the PV module in comparison with stand-alone one. Wang et al. [34] implemented a test to estimate the photo-to-thermal conversion performance of a PV/T unit between MXene@ water and graphene nanofluids. It is demonstrated that when the concentration is 20 ppm, the photo-to-thermal conversion efficiency of the MXene@ water achieves the maximum value of 63.35%.

Based on the aforementioned literature reviews, it is found that there are few studies on the performance assessment of a hybrid PV/T based on MXene nanomaterial combined with OF and a heat pump (HP) system. This paper supplies the research gap by investigating, in-depth, the PV/T combined OF and HP system energy production; the influences of the optical filtration channel height, concentration of the nanoparticles on PV surface temperature and overall system efficiency are also discussed. The heat transfer governing equations are determined based on the Version 11.349 Engineering Equation Solver (EES) software.

## 2. Energy Models

The system configuration comprises of an optical filtration (OF) channel, PV panel, solid/liquid MXene-enhanced phase change material layer, copper tube, EVA layer and adiabatic material layer as depicted in Figure 1. Specifically, the height of the OF channel is 1 cm which is directly attached to the front surface of a PV module. The solid MXene-PCM materials are filled in between the PV panel and the thermal copper pipes, which contributes to adjusting the temperature distribution of the PV array and increasing the heat transfer rate between the thermal pipe and thermal fluid.

The optical filtration (OF) channel is given as:

$$\alpha_g G = h_{g-am}(T_g - T_{am}) + h_{g-of}(T_g - T_{of}) \quad (1)$$

The convection heat transfer of the MXene-PCM nanofluid within the OF is written as:

$$\tau_g \alpha_{of} G = h_{of-g}(T_{of} - T_g) + h_{of-pv}(T_{of} - T_{pv}) + \frac{m_{of} \cdot c_{p_{of}}}{w} \frac{dT_{of}}{dx_1} \quad (2)$$

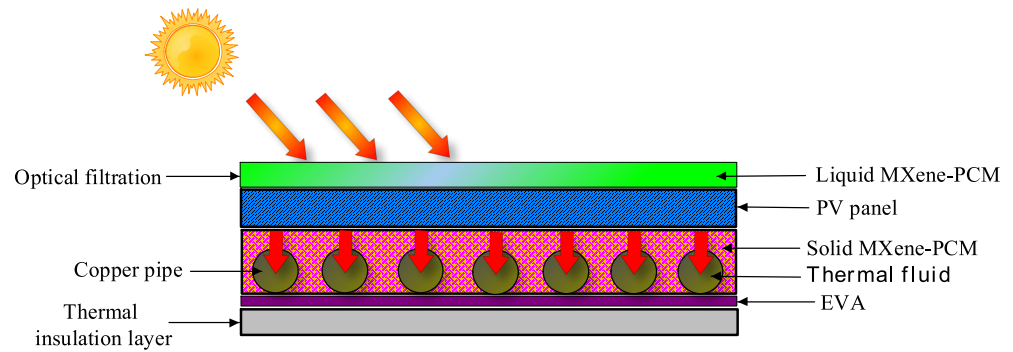


**Figure 1.** Diagram of PV/T with MXene-PCM module.

The PV module is expressed as:

$$\tau_g \tau_{of} \alpha_{pv} G = h_{pv-of} (T_{pv} - T_{of}) + \left( \frac{T_{pv} - T_b}{R_b} \right) + \eta_c \alpha_{pv} \tau_g \tau_{of} G \quad (3)$$

The conduction heat transfer of the solid MXene-PCM layer is given as:

$$\left( \frac{T_{pv} - T_b}{R_b} \right) = \lambda_{MXene-PCM} \frac{T_b - T_p}{\Delta t_{MXene-PCM}} \quad (4)$$

The convection heat transfer of thermal fluid within the thermal copper pipe is written as:

$$h_{p1-cf} (T_{p1} - T_{cf}) = h_{cf-p2} (T_{cf} - T_{p2}) + \frac{m_{cf} \cdot c_{p_{cf}}}{L} \frac{dT_{cf}}{dx_2} \quad (5)$$

For a PV/T system:

$$(\rho C_p V)_{PV/T} \frac{dT_{PV/T}}{dt} = (1 - \alpha_{glass}) G + Q_{conduction-1} - Q_{conduction-2} \quad (6)$$

$$Q_{conduction-1} = \frac{\lambda_{glass}}{\delta_{glass}} A_{glass} (T_{glass} - T_{PV/T}) \quad (7)$$

$$Q_{conduction-2} = \frac{\lambda_{PV/T}}{\delta_{PV/T}} A_{PV/T} (T_{PV/T} - T_{MXene-PCM}) \quad (8)$$

where  $\lambda_{PV/T}$  is the thermal conductivity;  $\delta_{PV/T}$  is the thickness.

$$Q_{tube} = \frac{\lambda_{tube}}{\delta_{tube}} A_{tube} (T_{MXene-PCM} - T_{tube}) = h_{MXene-PCM-fluid} A_{tube} (T_{tube} - T_{MXene-PCM-fluid}) = m \cdot C_{p_{MXene-PCM-fluid}} \Delta T_{MXene-PCM-fluid} \quad (9)$$

where  $Q_{tube}$  is the heat transfer to the system.

The phase change of governing equation is expressed as:

$$\rho_{MXene-PCM} C_{p_{MXene-PCM}} \frac{\partial T_{MXene-PCM}}{\partial t} = \frac{1}{dy} \int_{-y}^y \lambda_{MXene-PCM} \frac{\partial T_{MXene-PCM}}{\partial y} + \frac{1}{dx} \int_{-x}^x \lambda_{MXene-PCM} \frac{\partial T_{MXene-PCM}}{\partial x} \quad (10)$$

$$Q_{electricity} = LWCG \eta_{ref} [1 - \beta_{pv} (T_{pv} - T_{ref})]$$

The electrical output via the PV/T with nano-enhanced PCM unit is given as:

$$Q_{electricity} = LWCG \eta_{ref} [1 - \beta_{pv} (T_{pv} - T_{ref})] \quad (11)$$

The electrical efficiency is written as:

$$\eta_{electricity} = \frac{P_{electricity}}{P_{in}} = \eta_{ref} [1 - \beta_{pv} (T_{pv} - T_{ref})] \quad (12)$$

The thermal output via the PV/T with nano-enhanced PCM unit is illustrated as:

$$Q_{th} = m_{cf}c_{p,cf}(T_{cf,out} - T_{cf,in}) \tag{13}$$

$$\eta = \frac{Q_{th}}{P_{in}} \tag{14}$$

### 3. Description

#### 3.1. Weather Circumstance and Energy Requirements

As presented in Figure 2, the monthly highest mean temperature in Derby could reach 17.10 °C in July, while the lowest temperature is 4.4 °C in January. The monthly mean wind speed ranges from 3.9 m/s to 5.1 m/s. Additionally, the monthly average solar radiation and diffuse irradiation of Derby are in the range of 17.80 kWh/m<sup>2</sup> in December to 150 kWh/m<sup>2</sup> in June and from 11.3 kWh/m<sup>2</sup> in December to 87.3 kWh/m<sup>2</sup> in July, respectively.

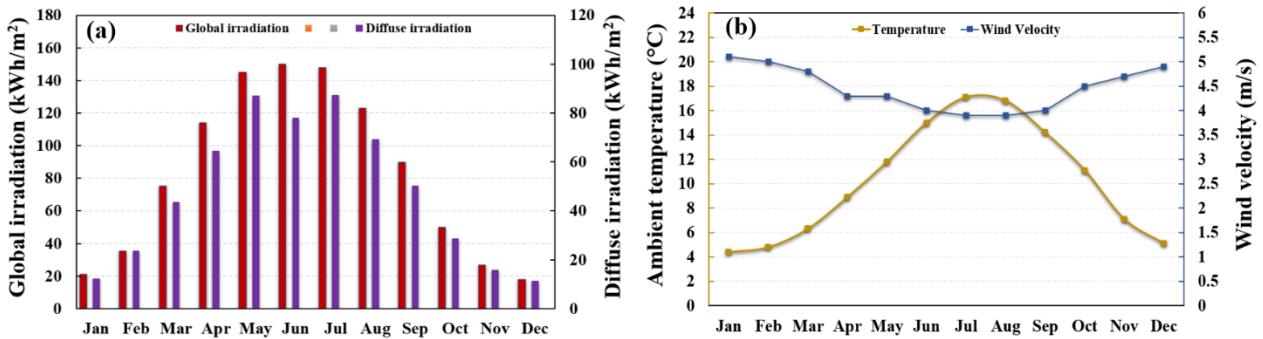


Figure 2. Weather circumstance: (a) global and diffuse irradiation; (b) air temperature and wind velocity in Derby, UK.

#### 3.2. Derby Office Building

The tested building office, as shown in Figure 3a, is called the Markeaton lodge and is situated at the University of Derby in Derbyshire.

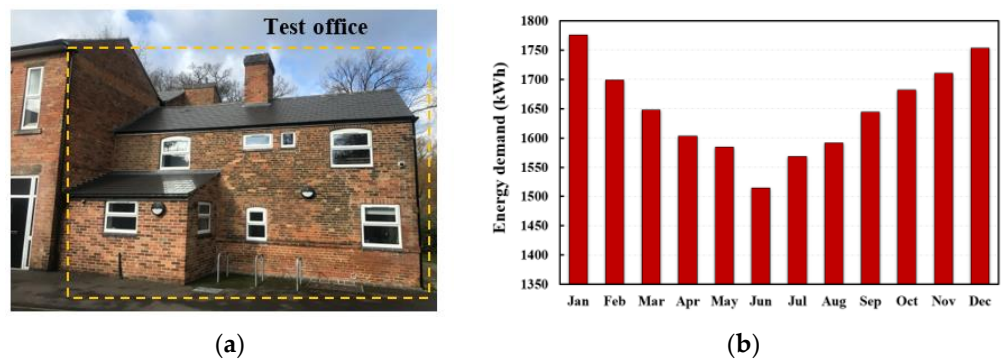


Figure 3. Weather circumstance: (a) global irradiation; (b) ambient air temperature and wind velocity in Derby, UK.

There are two floors with service and facilities within the building involving lecturer’s offices, postgraduate offices, a kitchen room and toilets for six-person utilization. The total floor area and southern side of the roof area are approximately 270 m<sup>2</sup> and 70.34 m<sup>2</sup>, respectively. Figure 3b describes the monthly building electrical and thermal energy needs. To be more specific, the largest and smallest energy requirements are 1776 kWh in January and 1515 kWh in June, and also the building’s entire energy demands reach 19,774 kWh per annum.

### 3.3. System Component

The project of the solar PV/T integrated with heat pump and OF system utilizes six (250Wp) CS6Pe250P PV modules with polycrystalline silicon from a Canadian solar company [35]. The thermal pipe has a diameter of 15mm, and the water flow rate within the pipe varies from 2 L/min to 6 L/min. Furthermore, the thermal pipe is connected to a 5.5 kW IVT Greenline heat pump [36]. The overall system component is simulated by using the Polysun software [37] as depicted in Figure 4, and the technical information is illustrated in Table 1.

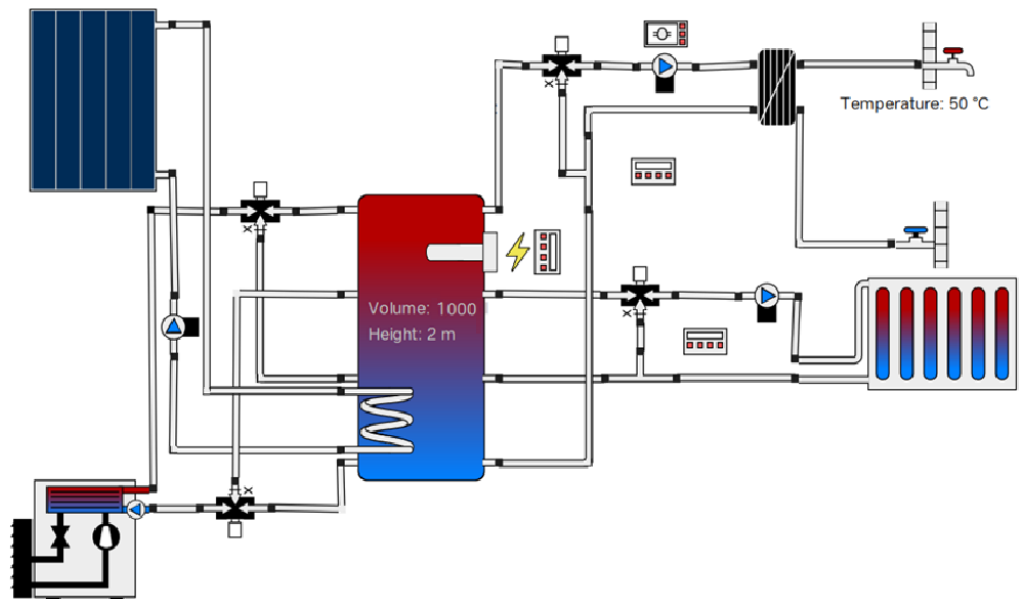


Figure 4. Diagram of system components.

Table 1. System parameters [35,36].

Item	Description	Value
PV/T module + OF	Optical filtration channel height	10 mm
	Make & Model	Canadian solar CS6P-250P
	Module dimension	1.6 × 0.98 × 0.04 m
	Number of PV modules	8
	Material	Polycrystalline silicon cell
	Peak Power	300 W
	Conversion efficiency	15.75%
	Maximum Voltage (V <sub>mpp</sub> )	37.60 V
	Maximum Current (I <sub>mpp</sub> )	8.10 A
	Weight of PV module	20.5 kg
	Title angle	25°
	Copper Thermal pipe thickness	2 mm
	MXene-PCM layer diameter	15 mm
Energy storage capacity of MXene-PCM	442.7 J/g	
EVA thickness	10 mm	
Insulation layer thickness	8 mm	
Heat pump	Emitted/Supplied output	6/1.8 kW
	Refrigerant R407C mass flow rate	0.02 kg/s
	Nominal flow heating medium	0.30 L/s
	Minimum flow heating medium	0.20 L/s

### 4. Results and Discussion

#### 4.1. Subsection PV/T Performance

The operating stage of the PV/T with the OF and HP system is divided into two periods on account of the Derby weather circumstances. It can be observed from Figure 5 that the maximum and minimum electrical energy production of PV/T with OF module is 706 kWh/monthly in June and 188 kWh/monthly in December, respectively. By comparison, the maximum and minimum electrical energy production of normal PV/T modules is 658 kWh in June and 157 kWh in December, respectively. The annual electrical energy obtained of PV/T with OF system could reach 5620 kWh which is greater, compared to the normal PV/T unit of 5085 kWh. Additionally, Figure 6 illustrates the average efficiency of PV modules during a one-year period; the annual average efficiency of PV/T with OF unit is about 14.65%, while the efficiency of normal PV/T unit is approximately 11.64%.

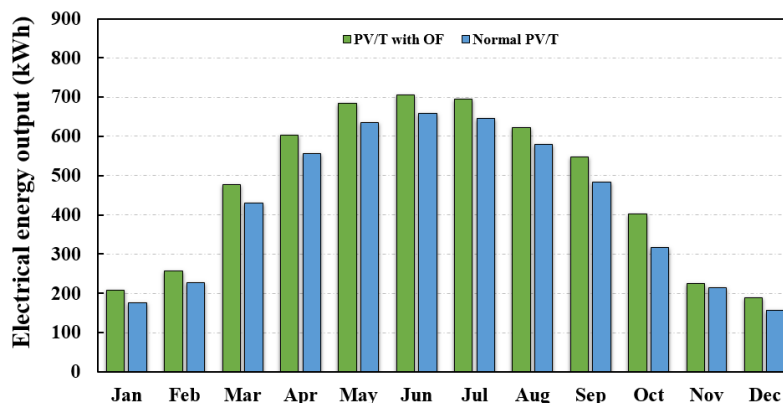


Figure 5. Electrical energy output.

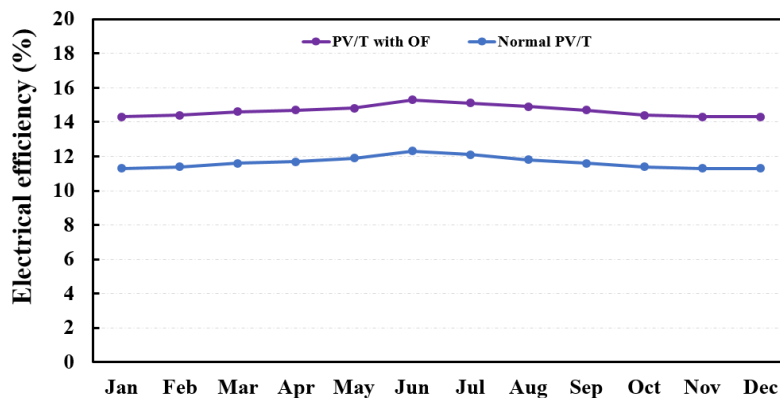


Figure 6. Electrical efficiency.

According to Figures 7 and 8, the thermal energy obtained from the PV/T with OF could reach the maximum and minimum values of 642 kWh with 74.92% thermal efficiency for June and 196 kWh with 37.33% thermal efficiency for December. By contrast, the thermal energy obtained of normal PV/T is up to 596 kWh with 71.88% efficiency for June and the minimum is 150 kWh with 33.3% efficiency for December. The entire heating from the PV/T with OF unit is 5370 kWh/year, which is higher in comparison with the normal one of 4818 kWh.

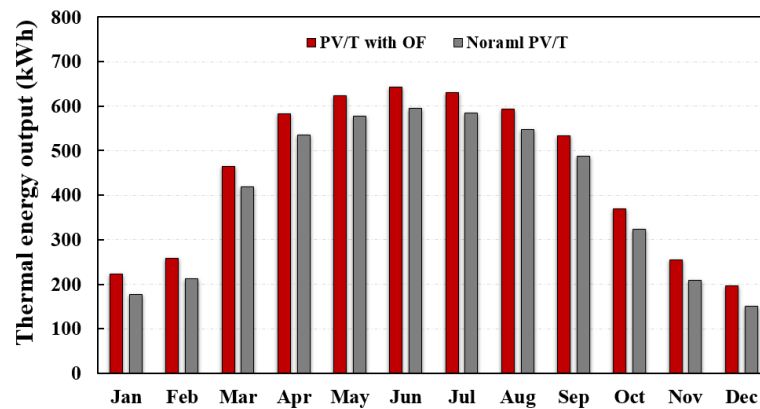


Figure 7. Thermal energy output.

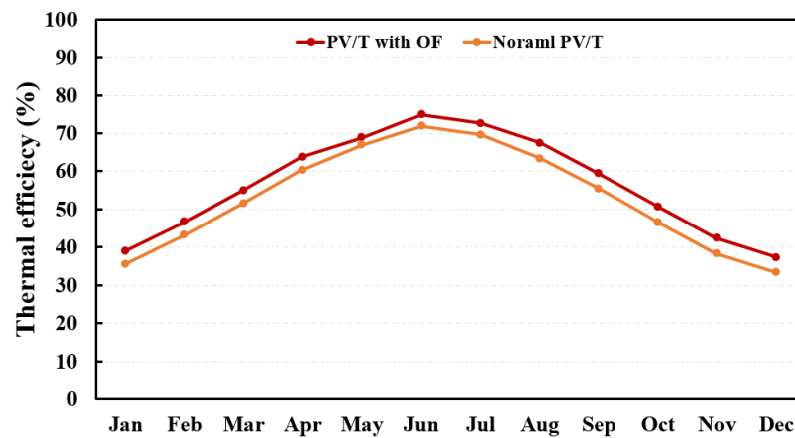


Figure 8. Thermal efficiency.

#### 4.2. Heat Pump Performance

The monthly mean heat pump electrical consumption and coefficient of performance (COP) are presented in Figures 9 and 10. The maximum and minimum monthly electrical consumption of PV/T with OF and HP are 512 kWh with COP of 5.18 for January and 29.8 kWh with COP of 4.44 for July, respectively. The overall electricity consumption of the PV/T with OF and HP system is 2251.2 kWh per annum, while the normal system is needed to consume the overall power of about 2963.2 kWh per annum. Meanwhile, the yearly COP of HP with OF could reach 4.94 which is greater than the normal HP of 3.83.

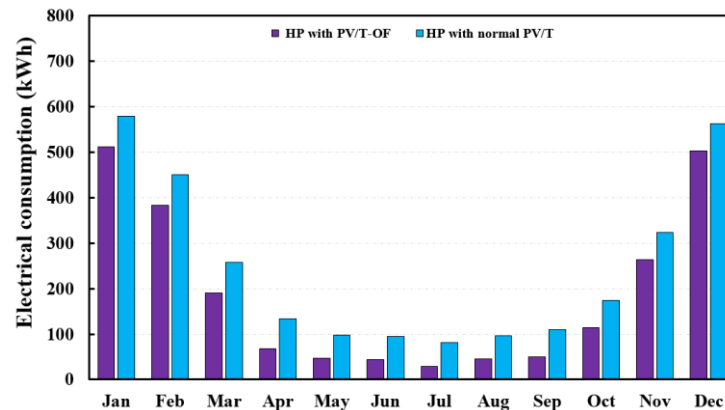


Figure 9. Electrical consumption of heat pump.

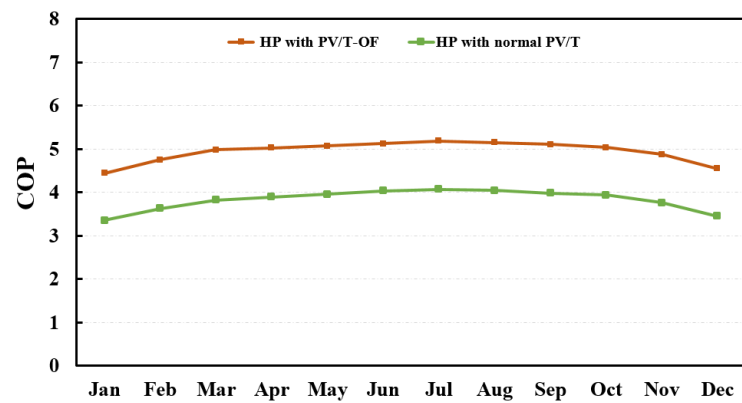


Figure 10. Heat pump COP.

#### 4.3. Effect of Optical Filtration Channel Height

It can be observed from Figure 11 that the height of the OF channel has a significant influence on thermal and electrical efficiencies. Specifically, the electrical efficiency is reduced from 14.6% to 14.3% with the height of the OF channel, on the contrary, the thermal efficiency is improved from 67.1% to 67.8% with the rising of the OF channel height.

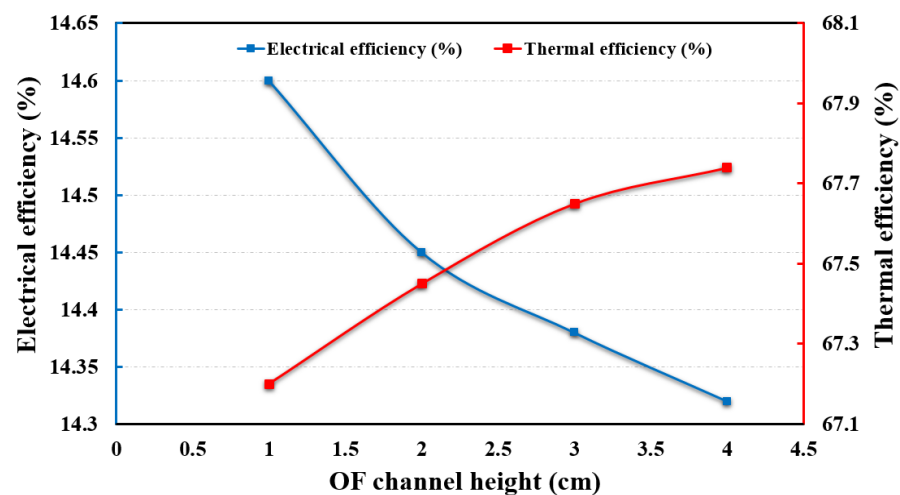


Figure 11. Influence of OF channel height on thermal and electrical efficiency.

In the calculating process, the mass flow rate of the thermal fluid is assumed as constant when the OF channel height is changed. The influences of the OF channel heights variation on the PV surface temperature and entire system efficiency are illustrated in Figure 12. To be more specific, the PV temperature increases from 35.2 °C to 39.3 °C when the OF channel height varies from 0.5 cm to 4 cm, indicating a negative influence of the OF channel height on the solar radiation absorption. Additionally, the overall system efficiency is almost kept constant, which is enhanced in the range from 81.2% to 83.3% when the OF channel height varies from 0.5 cm to 4 cm.

Moreover, the channel height and mass flow rate of thermal fluid are maintained at a constant value. It can be seen from Figure 13 that the volume concentration of the nano-enhanced PCM fluid in the OF exerts a negligible influence on the PV surface temperature, which is attributed to the air gap between the PV panel and OF channel and low mass flow rate in the OF. However, the overall system efficiency is enhanced when the volume concentration of the nanoparticles is increased in the range from 0.01 kg/s to 0.12 kg/s. This is because the low thermal resistance to heat losses and low radiation-shielding layers contributes to increasing the overall system efficiency.

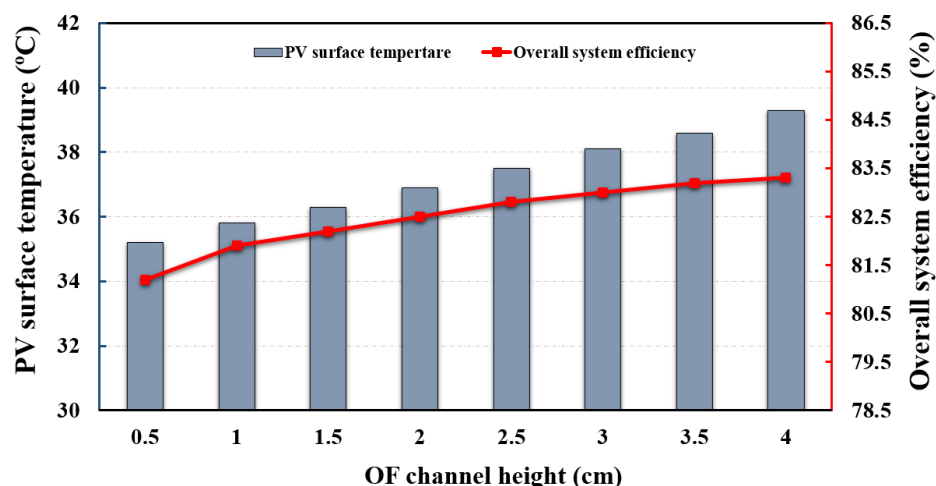


Figure 12. Influence of OF channel height variation.

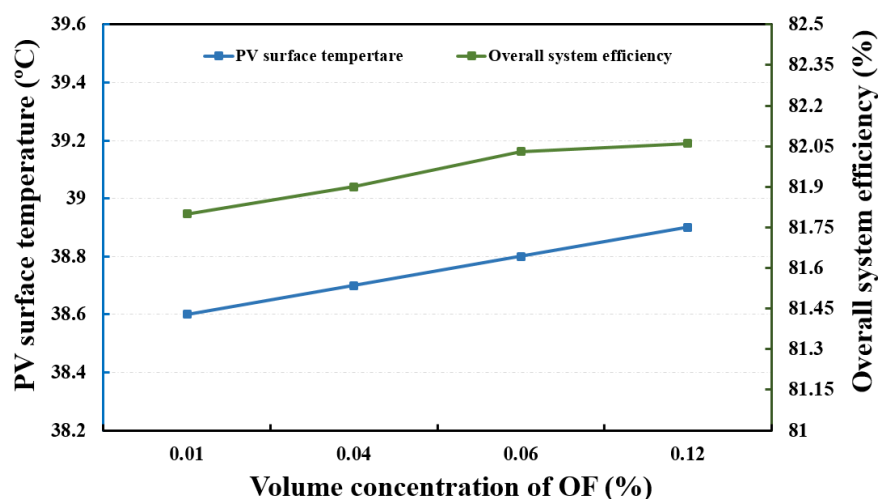


Figure 13. The effect of the OF channel height on the temperature of PV the module.

## 5. Conclusions

A numerical simulation has been performed to assess the improvement in the performance of a hybrid PV/T with optical filtration and the HP system, and the overall system components are established based on the Polysun software. The energy conversion efficiency of the PV/T with optical filtration and the HP system is compared with the normal system, meanwhile, the influences of the optical filtration channel height, concentration of the nanoparticles on PV surface temperature and overall system efficiency are discussed. The heat transfer governing equations are solved by using the EES software. Several vital conclusions are summarized in the following:

- OF is extremely effective at improving the whole PV/T unit performance.
- The electrical energy obtained from PV/T with an OF system could reach 5620 kWh/year with 14.65% power efficiency, which is higher compared to the normal PV/T system of 5085 kWh with 11.64% electrical efficiency.
- The thermal energy generation from the PV/T with OF unit is 5370 kWh/year with 74.92% efficiency, while the normal PV/T unit is only 4818 kWh with 71.88% efficiency.
- The yearly electricity consumption of the PV/T with OF and HP unit is 2251.2 kWh, by comparison, the normal system needed to consume an overall power of about 2963.2 kWh per annum. Meanwhile, the annual COP of the HP with OF could achieve 4.94 which is greater than the normal HP of 3.83.
- When the OF channel height is increased, it exerts an adverse effect on the PV surface temperature, but the overall thermal efficiency is enhanced.

- When the volume concentration of the nanofluid is boosted, the overall system efficiency is enhanced due to low thermal resistance to heat losses and low radiation-shielding layers.

**Author Contributions:** Conceptualization, Y.C., J.Z. and K.H.; Data curation, S.Z.; Writing—review & editing, H.T. All authors have read and agreed to the published version of the manuscript.

**Funding:** This research was funded by the Research on Dynamic Building Modularization, Grant Number: 2019CXR037.

**Institutional Review Board Statement:** Not applicable.

**Informed Consent Statement:** Not applicable.

**Data Availability Statement:** Not applicable.

**Conflicts of Interest:** The authors declare no conflict of interest.

## References

1. Dutta, R.; Chanda, K.; Maity, R. Future of solar energy potential in a changing climate across the world: A CMIP6 multi-model ensemble analysis. *Renew. Energy* **2022**, *188*, 819–829. [[CrossRef](#)]
2. Adedeji, A.R.; Zaini, F.; Mathew, S.; Dagar, L.; Petra, M.I.; Silva, L.C.D. Sustainable energy towards air pollution and climate change mitigation. *J. Environ. Manag.* **2020**, *260*, 109978. [[CrossRef](#)] [[PubMed](#)]
3. Rounis, E.D.; Athienitis, A.; Stathopoulos, T. Review of air-based PV/T and BIPV/T systems—Performance and modelling. *Renew. Energy* **2021**, *163*, 1729–1753. [[CrossRef](#)]
4. Huang, M.; Wang, Y.; Li, M.; Keovisar, V.; Li, X.; Kong, D.; Yu, Q. Comparative study on energy and exergy properties of solar photovoltaic/thermal air collector based on amorphous silicon cells. *Appl. Therm. Eng.* **2021**, *185*, 116376. [[CrossRef](#)]
5. Herrando, M.; Markides, C.N.; Hellgardt, K. A UK-based assessment of hybrid PV and solar-thermal systems for domestic heating and power: System performance. *Appl. Energy* **2014**, *122*, 288–309. [[CrossRef](#)]
6. Huang, C.; Sung, H.; Yen, K. Experimental study of photovoltaic/thermal (PV/T) hybrid system. *Int. J. Smart Grid Clean Energy* **2013**, *2*, 148–151. [[CrossRef](#)]
7. Bianchini, A.; Guzzini, A.; Pellegrini, M.; Saccani, C. Photovoltaic/thermal (PV/T) solar system: Experimental measurements, performance analysis and economic assessment. *Renew. Energy* **2017**, *111*, 543–555. [[CrossRef](#)]
8. Tang, X.; Quan, Z.; Zhao, Y. Experimental investigation of solar panel cooling by a novel micro heat pipe array. *Energy Power Eng.* **2010**, *2*, 171–174. [[CrossRef](#)]
9. Abdelrazik, A.S.; Al-Sulaiman, F.A.; Saidur, R. Feasibility study for the integration of optical filtration and nano-enhanced phase change materials to the conventional PV-based solar systems. *Renew. Energy* **2022**, *187*, 463–483. [[CrossRef](#)]
10. Abdelrazik, A.S.; Saidur, R.; Al-Sulaiman, F.A. Investigation of the performance of a hybrid PV/thermal system using water/silver nanofluid-based optical filter. *Energy* **2021**, *215*, 119172. [[CrossRef](#)]
11. Dejarnette, D.; Otanicar, T.; Brekke, N.; Hari, P.; Roberts, K.; Aaron, E. Plasmonic nanoparticle based spectral fluid filters for concentrating PV/T collectors. *Proc. SPIE Int. Soc. Opt. Eng.* **2014**, *9175*, 917509.
12. Han, X.; Xue, D.; Zheng, J.; Alelyani, S.M.; Chen, X. Spectral characterization of spectrally selective liquid absorption filters and exploring their effects on concentrator solar cells. *Renew. Energy* **2019**, *131*, 938–945. [[CrossRef](#)]
13. Abdelrazik, A.S.; Al-Sulaiman, F.A.; Saidur, R. Optical behavior of a water/silver nanofluid and their influence on the performance of a photovoltaic-thermal collector. *Sol. Energy Mater. Sol. Cells* **2019**, *201*, 110054. [[CrossRef](#)]
14. Al-Waeli, A.H.A.; Sopian, K.; Chaichan, M.T.; Kazem, H.A.; Ibrahim, A.; Mat, S.; Ruslan, M.H. Evaluation of the nanofluid and nano PCM based photovoltaic thermal (PVT) system: An experimental study. *Energy Convers. Manag.* **2017**, *151*, 693–708. [[CrossRef](#)]
15. Al-Waeli, A.H.A.; Sopian, K.; Chaichan, M.T.; Kazem, H.A.; Ibrahim, A.; Mat, S.; Ruslan, M.H. Comparison of prediction methods of PV/T nanofluid and nano-PCM system using a measured dataset and artificial neural network. *Sol. Energy* **2018**, *162*, 378–396. [[CrossRef](#)]
16. Aberoumand, S.; Ghamari, S.; Shabani, B. Energy and exergy analysis of a photovoltaic thermal (PV/T) system using nanofluids: An experimental study. *Sol. Energy* **2018**, *165*, 167–177. [[CrossRef](#)]
17. Han, X.; Chen, X.; Wang, Q.; Alelyani, S.M.; Qu, J. Investigation of CoSO<sub>4</sub>-based Ag nanofluids as spectral beam splitters for hybrid PV/T applications. *Sol. Energy* **2019**, *177*, 387–394. [[CrossRef](#)]
18. Dehaj, M.S.; Mohiabadi, M.Z. Experimental investigation of heat pipe solar collector using MgO nanofluids. *Sol. Energy Mater. Sol. Cells* **2019**, *191*, 91–99. [[CrossRef](#)]
19. Sharafeldin, M.A.; Gróf, G. Evacuated tube solar collector performance using CeO<sub>2</sub>/water nanofluid. *J. Clean. Prod.* **2018**, *185*, 347–356. [[CrossRef](#)]
20. Sharafeldin, M.A.; Gróf, G. Efficiency of evacuated tube solar collector using WO<sub>3</sub>/Water nanofluid. *Renew. Energy* **2019**, *134*, 453–460. [[CrossRef](#)]

21. Ebaid, M.S.Y.; Ghrair, A.M.; Al-Busoul, M. Experimental investigation of cooling photovoltaic (PV) panels using (TiO<sub>2</sub>) nanofluid in water -polyethylene glycol mixture and (Al<sub>2</sub>O<sub>3</sub>) nanofluid in water- cetyltrimethylammonium bromide mixture. *Energy Convers. Manag.* **2018**, *55*, 324–343. [[CrossRef](#)]
22. Sardarabadi, M.; Hosseinzadeh, M.; Kazemian, A.; Passandideh-Fard, M. Experimental investigation of the effects of using metal-oxides/water nanofluids on a photovoltaic thermal system (PVT) from energy and exergy viewpoints. *Energy* **2017**, *138*, 682–695. [[CrossRef](#)]
23. Eidan, A.A.; AlSahlani, A.; Ahmed, A.Q.; Al-fahham, M.; Jalil, J.M. Improving the performance of heat pipe-evacuated tube solar collector experimentally by using Al<sub>2</sub>O<sub>3</sub> and CuO/acetone nanofluids. *Sol. Energy* **2018**, *173*, 780–788. [[CrossRef](#)]
24. Mercan, M.; Yurddaş, A. Numerical analysis of evacuated tube solar collectors using nanofluids. *Sol. Energy* **2019**, *191*, 167–179. [[CrossRef](#)]
25. Al-Waeli, A.H.A.; Chaichan, M.T.; Kazem, H.A.; Sopian, K. Comparative study to use nano-(Al<sub>2</sub>O<sub>3</sub>, CuO, and SiC) with water to enhance photovoltaic thermal PV/T collectors. *Energy Convers. Manag.* **2017**, *148*, 963–973. [[CrossRef](#)]
26. Yuan, W.; Ji, J.; Modjinou, M.; Zhou, F.; Li, Z.; Song, Z.; Huang, S.; Zhao, X. Numerical simulation and experimental validation of the solar photovoltaic/thermal system with phase change material. *Appl. Energy* **2018**, *232*, 715–727. [[CrossRef](#)]
27. Al-Waeli, A.H.A.; Chaichan, M.T.; Kamaruzzaman, S.; Kazem, H.A.; Mahood, H.B.; Khadom, A.A. Modeling and experimental validation of a PVT system using nanofluid coolant and nano-PCM. *Sol. Energy* **2019**, *177*, 178–191. [[CrossRef](#)]
28. Al-Waeli, A.H.A.; Kazem, H.A.; Chaichan, M.T.; Kamaruzzaman, S. Experimental investigation of using nano-PCM/nanofluid on a photovoltaic thermal system (PVT): Technical and economic study. *Therm. Sci. Eng. Prog.* **2019**, *11*, 213–223. [[CrossRef](#)]
29. Mao, H.; Gu, C.; Yan, S.; Xin, Q.; Cheng, S.; Tan, P.; Wang, X.; Xiu, F.; Liu, X.; Liu, J.; et al. MXene Quantum dot/polymer hybrid structures with tunable electrical conductance and resistive switching for nonvolatile memory devices. *Adv. Electron. Mater.* **2020**, *6*, 1900493. [[CrossRef](#)]
30. Lim, G.P.; Soon, C.F.; Morsin, M.; Ahmad, M.K.; Nayan, N.; Tee, K.S. Synthesis, characterization and antifungal property of Ti<sub>3</sub>C<sub>2</sub>T<sub>x</sub> MXene nanosheets. *Ceram. Int.* **2020**, *46*, 20306–20312. [[CrossRef](#)]
31. Fan, X.; Liu, L.; Jin, X.; Wang, W.; Zhang, S.; Tang, B. MXene Ti<sub>3</sub>C<sub>2</sub>T<sub>x</sub> for phase change composite with superior photothermal storage capability. *J. Mater. Chem. A* **2019**, *7*, 14319–14327. [[CrossRef](#)]
32. Mo, Z.; Mo, P.; Yi, M.; Hu, Z.; Tan, G.; Selim, M.S.; Chen, Y.; Chen, X.; Hao, Z.; Wei, X. Ti<sub>3</sub>C<sub>2</sub>T<sub>x</sub>@ Polyvinyl alcohol foam-supported phase change materials with simultaneous enhanced thermal conductivity and solar-thermal conversion performance. *Sol. Energy Mater. Sol. Cells* **2021**, *219*, 110813. [[CrossRef](#)]
33. Samylingam, L.; Aslfattahi, N.; Saidur, R.; Yahya, S.M.; Afzal, A.; Arifutzzaman, A.; Tan, K.H.; Kadirgama, K. Thermal and energy performance improvement of hybrid PV/T system by using olein palm oil with MXene as a new class of heat transfer fluid. *Sol. Energy Mater. Sol. Cells* **2020**, *218*, 110754. [[CrossRef](#)]
34. Wang, H.; Li, X.; Luo, B.; Wei, K.; Zeng, G. The MXene/water nanofluids with high stability and photo-thermal conversion for direct absorption solar collectors: A comparative study. *Energy* **2021**, *227*, 120483. [[CrossRef](#)]
35. CS6P-250P (250W) Solar Panel. Available online: <https://www.zonnepanelen.net/nl/pdf/panels/CS6P-Pen.pdf> (accessed on 1 July 2016).
36. IVT Greenline HT Plus. Available online: <http://www.varmepumpservice.se/LinkClick.aspx?fileticket=x3oH4kK01So%3D&tabid=1954> (accessed on 1 September 2008).
37. Witzig, A.; Stöckli, U.; Kistler, P.; Bornatico, R.; Pfeiffer, M. Polysun inside: A universal platform for commercial software and research applications. In Proceedings of the EuroSun 2010, International Conference on Solar Heating, Cooling and Buildings, Graz, Austria, 28 September–1 October 2010.